NATIONAL ADVISORY COMMITTEE FOR AERONAUTICS

TECHNICAL NOTE

No. 1295

WIND-TUNNEL INVESTIGATION OF THE AIR LOAD DISTRIBUTION ON TWO COMBINATIONS OF LIFTING SURFACE AND FUSELAGE

By Carl A. Sandahl and Samuel D. Vollo

Langley Memorial Aeronautical Laboratory
Langley Field, Va.

Washington
May 1947

NATIONAL ADVISORY COMMITTEE FOR AERONAUTICS

TECHNICAL NOTE NO. 1295

WIND-TUNNEL INVESTIGATION OF THE AIR LOAD DISTRIBUTION ON TWO COMBINATIONS OF LIFTING SURFACE AND FUSELAGE

By Carl A. Sandahl and Samuel D. Vollo

SUMMARY

Wind-tunnel measurements have been made of the air load distribution on a canard-type model. Two combinations of lifting surface and fuselage, representing appreciable variation of lifting-surface span relative to fuselage diameter, were obtained by removing separately the wing and stabilizer of the model. The tests also included measurements of lift, drag, and pitching moment for several configurations. The results show that, for the configurations tested, the spanwise loadings on the combinations agreed fairly well with the loadings calculated by Lennertz's method.

INTRODUCTION

A theoretical approach to the problem of lifting-surface-fuselage interference is given in reference 1 in which the spanwise loading is obtained for a lifting line intersecting the center line of an infinitely long circular cylinder. This analysis predicts a decrease in the spanwise loading over the fuselage and a reduction in total lift as compared with the spanwise loading and lift of the wing alone at the same angle of attack. Measurements of the lift of a large number of wing-fuselage combinations (reference 2) indicate, however, that the lift of the wing-fuselage combination is more nearly equal to the lift of the wing alone. Over-all lift measurements of wings and wing-fuselage combinations, however, do not define the spanwise load curve. The purpose of the present investigation is to present data relating to the measured and calculated spanwise loadings on two combinations of lifting surface and fuselage having appreciable variation of span relative to fuselage diameter. The tests included measurements of pressure distribution, lift, drag, and pitching moment for several model configurations over a range of angles of attack at several yaw angles.

SYMBOLS

P	pressure coefficient $\left(\frac{p - p_o}{q_o}\right)$
$\frac{d(N/q_o)}{dy}$	section load derivative for horizontal surfaces
C_N	normal-force coefficient (N/q_oS)
C_L	lift coefficient (L/q_oS)
C_D	total drag coefficient (D/q_oS)
C_{D_o}	profile-drag coefficient (D_o/q_oS)
C_{D_s}	drag coefficient based on stabilizer area (D/q_oS_S)
C_{L_s}	lift coefficient based on stabilizer area (L/q_oS_S)
C_m	pitching-moment coefficient $(M/q_oS\bar{c})$
p	local static pressure
p_o	free-stream static pressure
q_o	free-stream dynamic pressure
N	normal force
L	lift
D	total drag
D_o	profile drag
S	wing area (19.86 sq ft)
S_s	stabilizer area (4.06 sq ft)
$\bar{c}$	wing mean aerodynamic chord (1.87 ft)
c	local wing chord
b	wing span (11.00 ft)
b_s	stabilizer span (4.62 ft)

A	aspect ratio
l	fuselage length (15.98 ft)
α	angle of attack, degrees
ψ	angle of yaw, positive when nose is displaced to right, degrees
ϕ	angular position of generatrix of fuselage body of revolution, measured from the vertical plane of symmetry, degrees
d	fuselage diameter at quarter chord of wing
d_s	fuselage diameter at quarter chord of stabilizer
x	longitudinal coordinate parallel to fuselage center line
y	lateral coordinate perpendicular to plane of symmetry
z	vertical coordinate perpendicular to x,y plane

APPARATUS AND TESTS

The test model used was constructed of plywood and was finished to a fair aerodynamic surface. The general arrangement of the model is shown in figure 1. The wing, stabilizer, and vertical tail were removable from the fuselage, which was a body of revolution. All control surfaces were set at neutral and the gaps were sealed for this investigation.

The model was mounted in the Langley propeller-research tunnel on the six-component-balance system as shown in figure 2. The model was attached at the center of gravity to a single support strut by means of a universal fitting which permitted the setting of pitch and yaw angles. Motion in pitch was restrained by a "nose" wire, the lower end of which was attached to a balance to allow the measurement of pitching moments. The tunnel balance system was used to measure lift and drag.

The pressure distribution on the fuselage was obtained by orifices flush with the surface and arranged as shown in figure 1. Chordwise pressure distributions on the right wing panel and the

left stabilizer panel were measured by means of pressure belts. On the basis of the results reported in references 3 and 4, the belt method of pressure-distribution measurement is considered to be of sufficient accuracy for the present investigation.

The investigation consisted of measurements of lift, drag, pitching moment, and pressure distributions over a range of angles of attack from -2° to 16° and at angles of yaw of $\pm 10^\circ$, $\pm 5^\circ$, and 0°. The unsymmetric distribution of fuselage orifices necessitated tests at equal positive and negative angles of yaw in order to obtain complete fuselage pressure distributions. At zero yaw, the pressures at points at equal angular displacement from the vertical plane of symmetry are considered to be equal. The following configurations were tested and are designated herein as follows:

Configuration	Designation
Fuselage with wing, stabilizer, and vertical tail	FWST
Fuselage with wing and vertical tail	FWT
Fuselage with wing	FW
Fuselage with stabilizer and vertical tail	FST
Fuselage alone	F

The test velocity was varied from 80 to 100 miles per hour corresponding to a Reynolds number range from 1.4 to 1.7×10^6 based on the wing mean aerodynamic chord of 1.87 feet.

RESULTS

The results are presented in figures 3 to 10. Corrections for jet-boundary effects have been applied to the angle of attack and the drag coefficient. The tare drag was estimated and has been applied to the measured drag.

The fuselage pressure distribution for different angles of attack and yaw for configurations F and FWST are shown in figures 3 to 5. The pressure distributions for the various positions of the generatrix of the fuselage were obtained by

cross-plotting the pressure distributions measured at the various longitudinal stations of the fuselage. The pressure distributions in the plane of symmetry for configurations F, FST, and FW are given in figure 6.

The spanwise loading curves for the wing and stabilizer are given in figures 7 and 8. Outboard of the fuselage the section load derivative $\frac{d(N/q_o)}{dy}$ was obtained by integrating chordwise pressure distributions measured at three stations along the semispans of the wing and stabilizer. The fuselage section loadings induced by the wing were obtained by superimposing fuselage pressure-distribution curves for configurations F and FW drawn for the vertical plane of symmetry and for a parallel plane displaced 5 inches. The total difference in the areas of the pressure diagrams for the two configurations was then used in computing the section load derivative $\frac{d(N/q_o)}{dy}$. An identical procedure utilizing configurations F and FST was used in computing the load induced on the fuselage by the stabilizer.

The variation of lift, drag, and pitching-moment coefficients with angle of attack for several configurations is shown in figure 9. Measurements for configuration FST at $\psi = 0^\circ$ are not available; the curves for this configuration were obtained by extrapolating tests at $\psi = \pm 5^\circ$ and $\pm 10^\circ$. The coefficients are based on wing dimensions regardless of configuration.

DISCUSSION

Fuselage pressure distribution.- Although isolation of the effects of the individual components is not possible, the general manner in which the lifting surfaces affect the distribution of pressure on the fuselage is shown in figures 3 to 5. In general, the main effects of the wing or stabilizer are limited to the immediate vicinity of the fuselage junctures of the wing and stabilizer. The distance along the fuselage over which the fuselage pressure distribution is materially affected by either the wing or stabilizer is shown more clearly in figure 6 to be approximately a distance of one chord ahead of the leading edge and one chord behind the trailing edge of each of the components. Defining these limits is difficult, inasmuch as the pressure-distribution curves for the different configurations are asymptotic.

Spanwise loadings.- The measured and calculated spanwise load distributions are shown in figures 7 and 8. The spanwise load distributions predicted by the theory (reference 1) are in agreement with the measured spanwise load distributions. The agreement was particularly good for the configuration FST, for which the conditions assumed in deriving the theory were more nearly fulfilled. In deriving the theory, the fuselage is assumed to be infinite in length and at zero angle of attack, the wing axis and fuselage axis are assumed to intersect, and the loading is considered to be such that the induced drag is a minimum. In addition, the wing chord should be comparatively small with respect to the span and the fuselage diameter should not be small in comparison with the wing chord. It has been suggested from theoretical considerations that the loss in load over the lifting-surface in the vicinity of the fuselage would be regained on the fuselage, where it is tapered to finite length; however, no such increase in load over the rear of the fuselage was measured in these tests, probably because of fuselage boundary-layer effects. Evidence of appreciable fuselage boundary layer is indicated by the pressure-distribution curves of configuration F (fig. 6(a)), which show that almost no negative lift is developed over the rear of the fuselage. This lack of negative lift over the rear of the fuselage probably accounts, in part, for the lack of agreement between the calculated and measured pitching-moment coefficients of figure 9. The calculated pitching-moment coefficients in this figure for configuration F were made by the method of reference 5.

Induced drag.- The induced-drag coefficients associated with the measured spanwise loadings on the wing and stabilizer were computed by the method of reference 6 and are shown in figure 10. Substantially the same induced-drag coefficients were obtained from a 6-point and a 10-point Fourier series determination; thus, a sufficient number of points were indicated to have been utilized in the analysis.

A comparison (fig. 10(a)) of the induced-drag coefficient computed from the measured spanwise loadings on the wing-fuselage combination and the minimum induced-drag coefficient for the combination computed from the method of reference 1 indicates a reduction in effective aspect ratio of 19 percent as a result of distortion of the measured spanwise load distribution from the ideal load distribution for the combination. Good agreement exists between the induced-drag coefficient obtained from the force tests and from the measured spanwise loadings.

A similar comparison (fig. 10(b)) for the stabilizer-fuselage combination indicates exact agreement between the

induced-drag coefficient computed from the measured spanwise loadings and computed from reference 1. The exact agreement for this configuration results from the good agreement between the measured and calculated spanwise load distributions.

CONCLUSIONS

Results of an experimental investigation to determine the spanwise loading for several combinations of fuselage and lifting surface showed reasonable agreement between the measured loadings and the calculated loadings obtained by Lennertz's method.

Langley Memorial Aeronautical Laboratory
National Advisory Committee for Aeronautics
Langley Field, Va., February 19, 1947

REFERENCES

1. Lennertz, J.: Influence of the Airplane Body on the Wings. Vol. IV of Aerodynamic Theory, div. K, ch. III, sec. 1, W. F. Durand, ed., Julius Springer (Berlin), 1935, pp. 152-157.

2. Jacobs, Eastman N., and Ward, Kenneth E.: Interference of Wing and Fuselage from Tests of 209 Combinations in the N.A.C.A. Variable-Density Tunnel. NACA Rep. No. 540, 1935.

3. Corson, Blake W., Jr.: The Belt Method for Measuring Pressure Distribution. NACA RB, Feb. 1943.

4. Zalovcik, John A., and Daum, Fred L.: Flight Investigation at High Mach Numbers of Several Methods of Measuring Static Pressure on an Airplane Wing. NACA RB No. L4H10a, 1944.

5. Munk, Max M.: The Aerodynamic Forces on Airship Hulls. NACA Rep. No. 184, 1924.

6. Glauert, H.: The Elements of Aerofoil and Airscrew Theory. Cambridge Univ. Press, 1926, pp. 139-140.

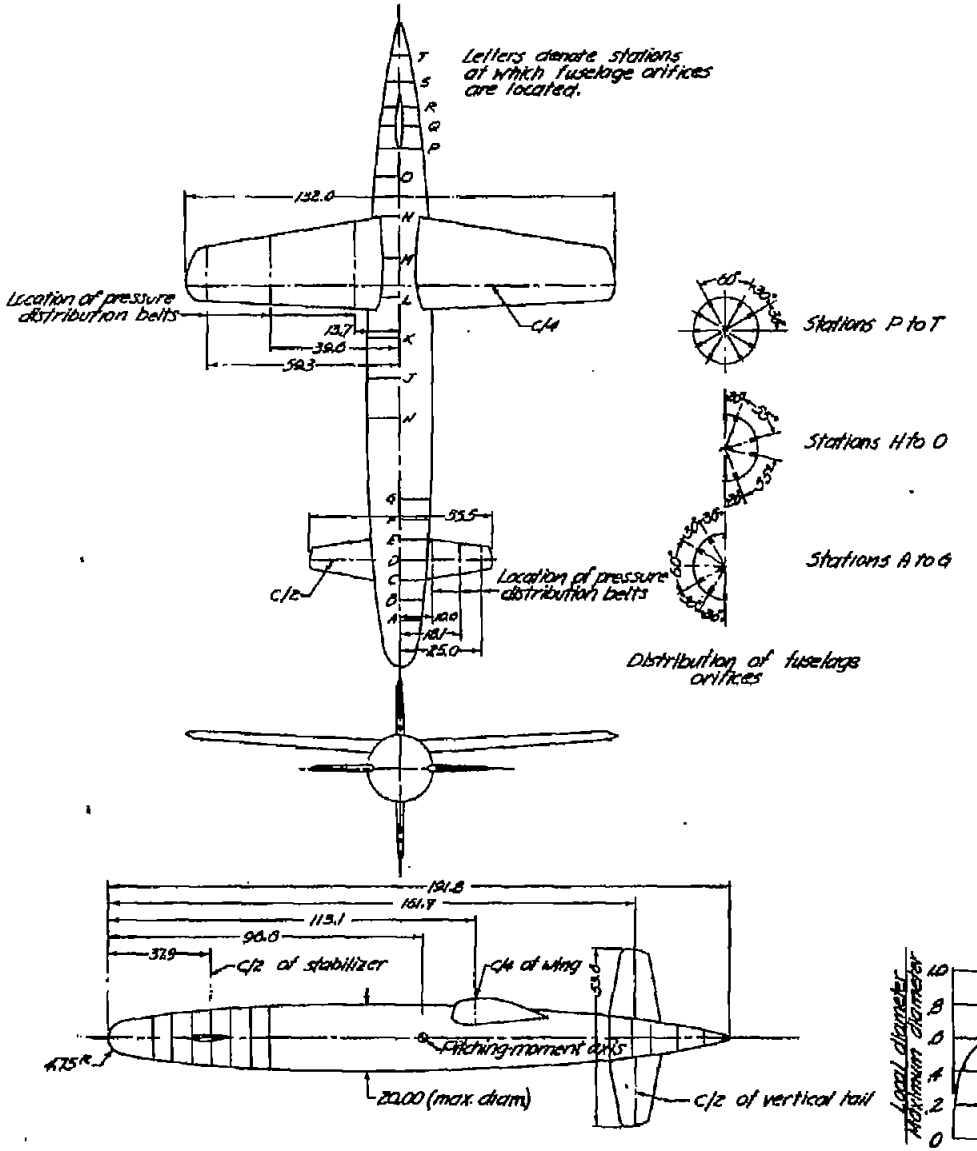

Distribution of fuselage orifices

Wing	
Airfoil (root to tip)	NACA 66,2-016
Tip chord, in.	14.40
Root chord, in.	31.10
Area, sq ft	19.86
Geometric twist, deg	0
Aspect ratio	6.09
Incidence, deg	1.0
Dihedral, deg	4.0
M.A.C.	22.4

Stabilizer	
Airfoil (root to tip)	NACA 66,2-012
Tip chord, in.	6.00
Root chord, in.	12.32
Area, sq ft	4.06
Geometric twist, deg	0
Aspect ratio	5.27
Incidence, deg	-0.7
Dihedral, deg	0.

Vertical tail	
Airfoil (root to tip)	66,2-015
Tip chord	7.94
Root chord (5.75" from ℄)	18.40
Area, sq ft	4.90
Aspect ratio	2.05

Dimensions of all aerodynamic surfaces obtained by extending the leading and trailing edges to plane of symmetry

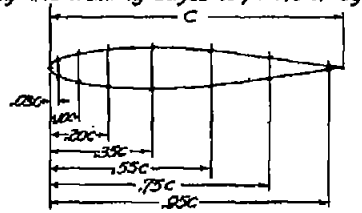

Chordwise distribution of orifices for all pressure distribution belts

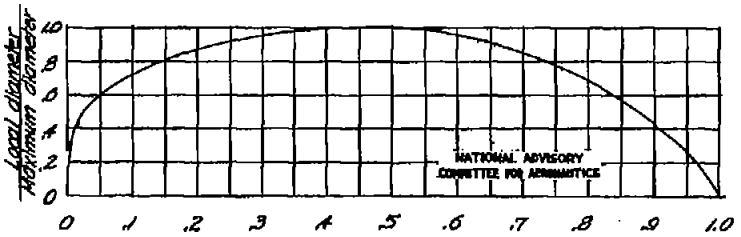

Fuselage thickness distribution

Figure 1.- Geometric details of model. (All dimensions not specified are in inches.)

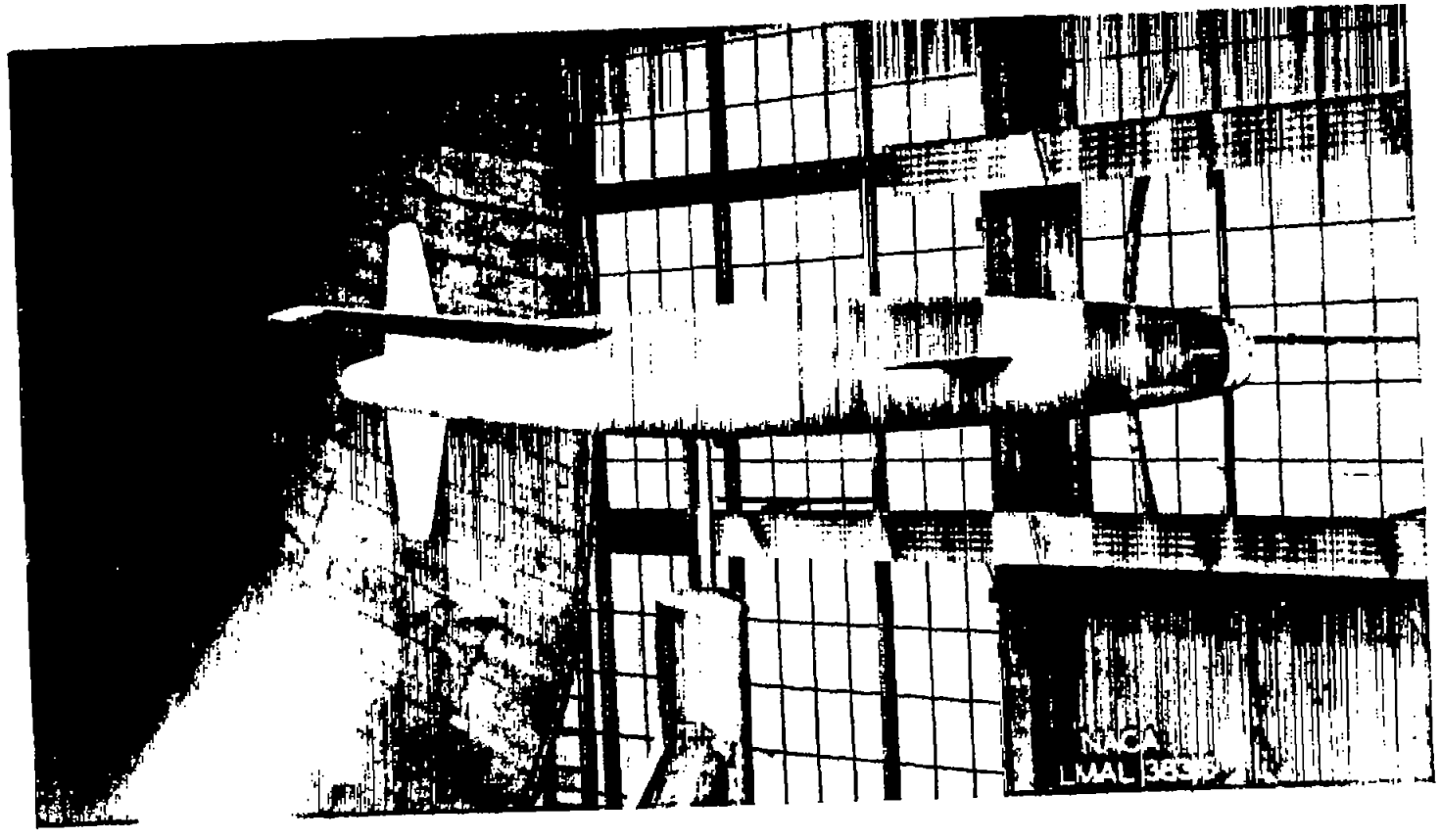

(a) Configuration FWST.

Figure 2.- Model installed for testing.

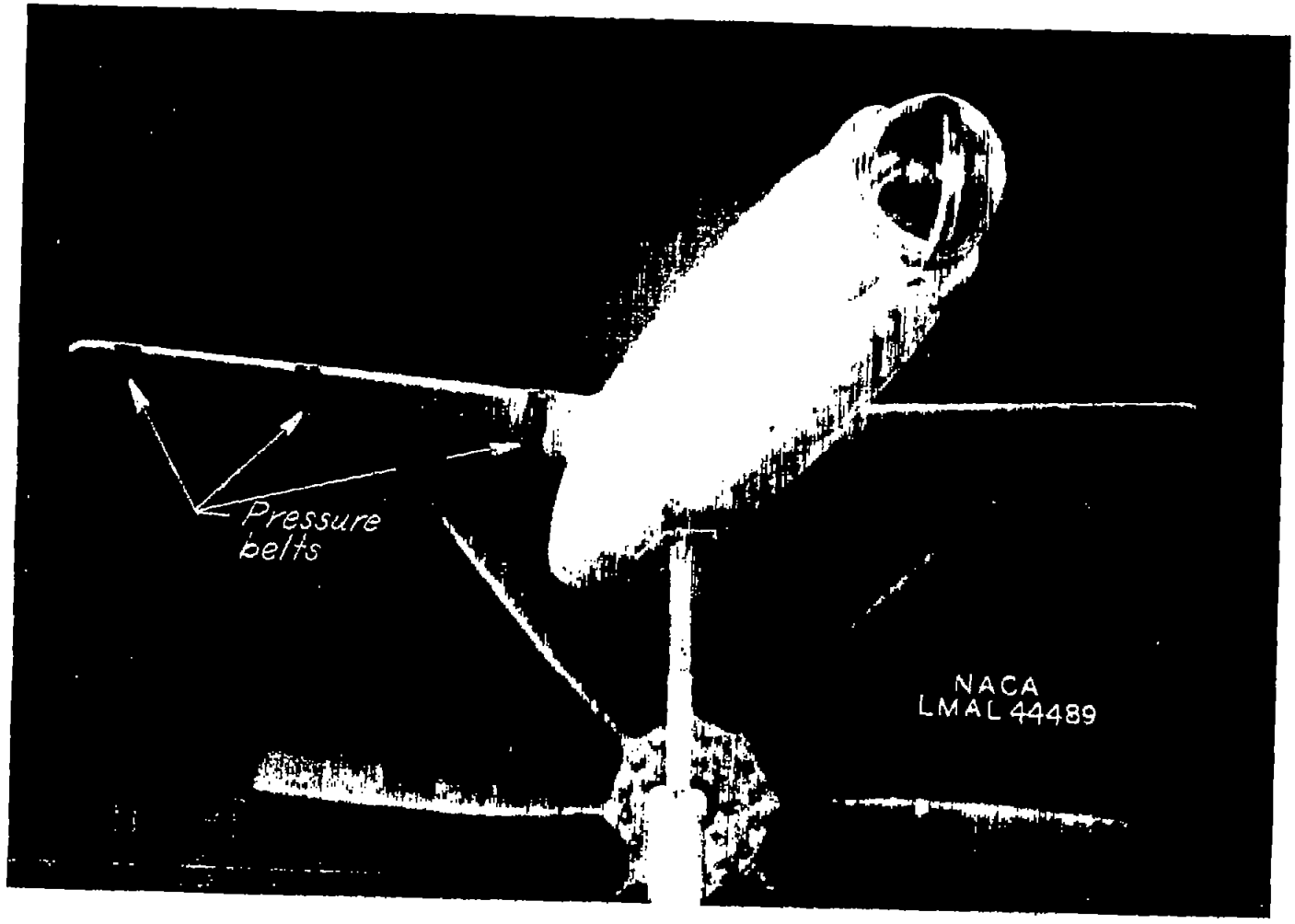

(b) Configuration FW.

Figure 2.- Concluded.

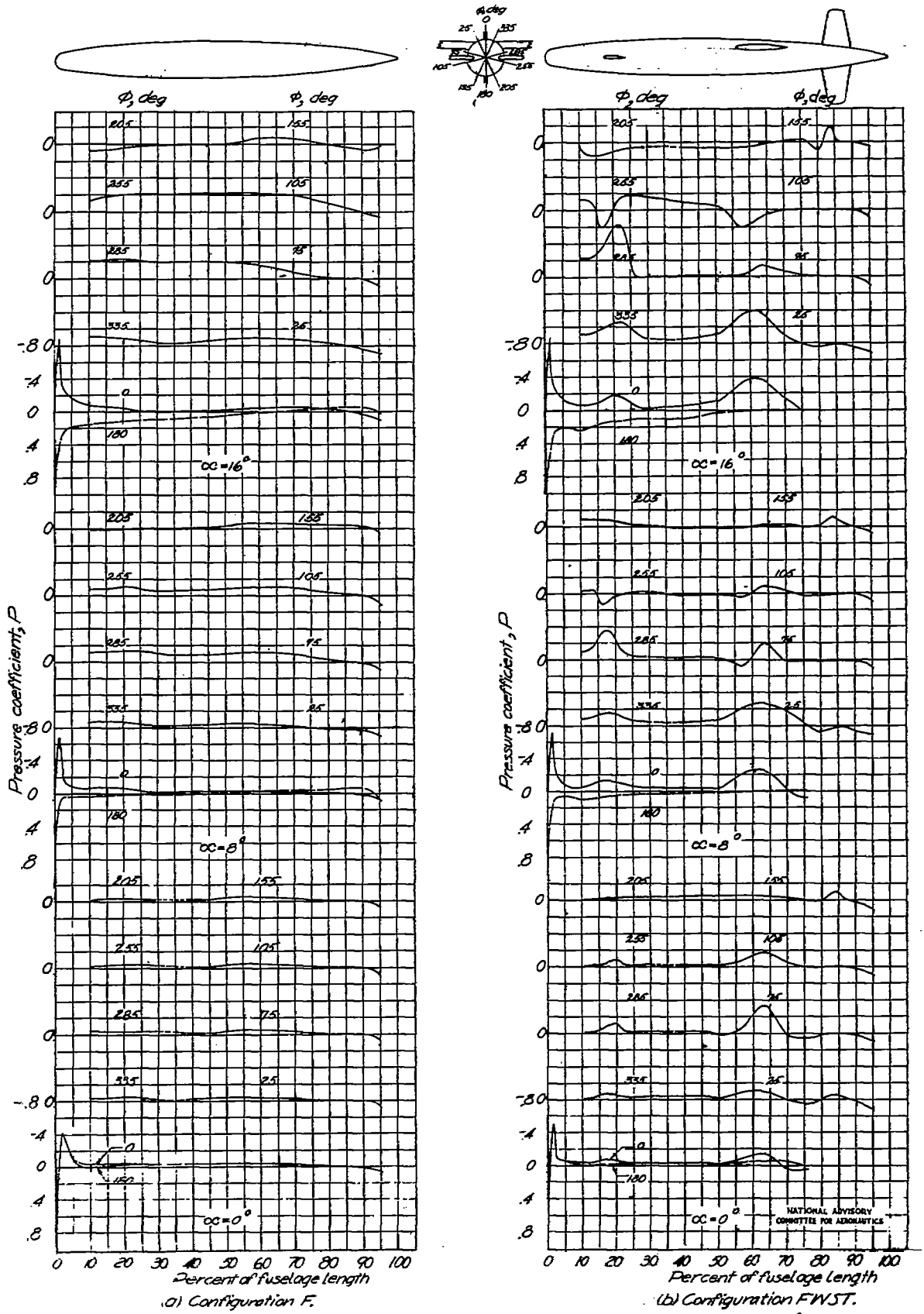

Figure 3 - Fuselage pressure distribution for several positions of the generatrix. $\psi = 0°$.

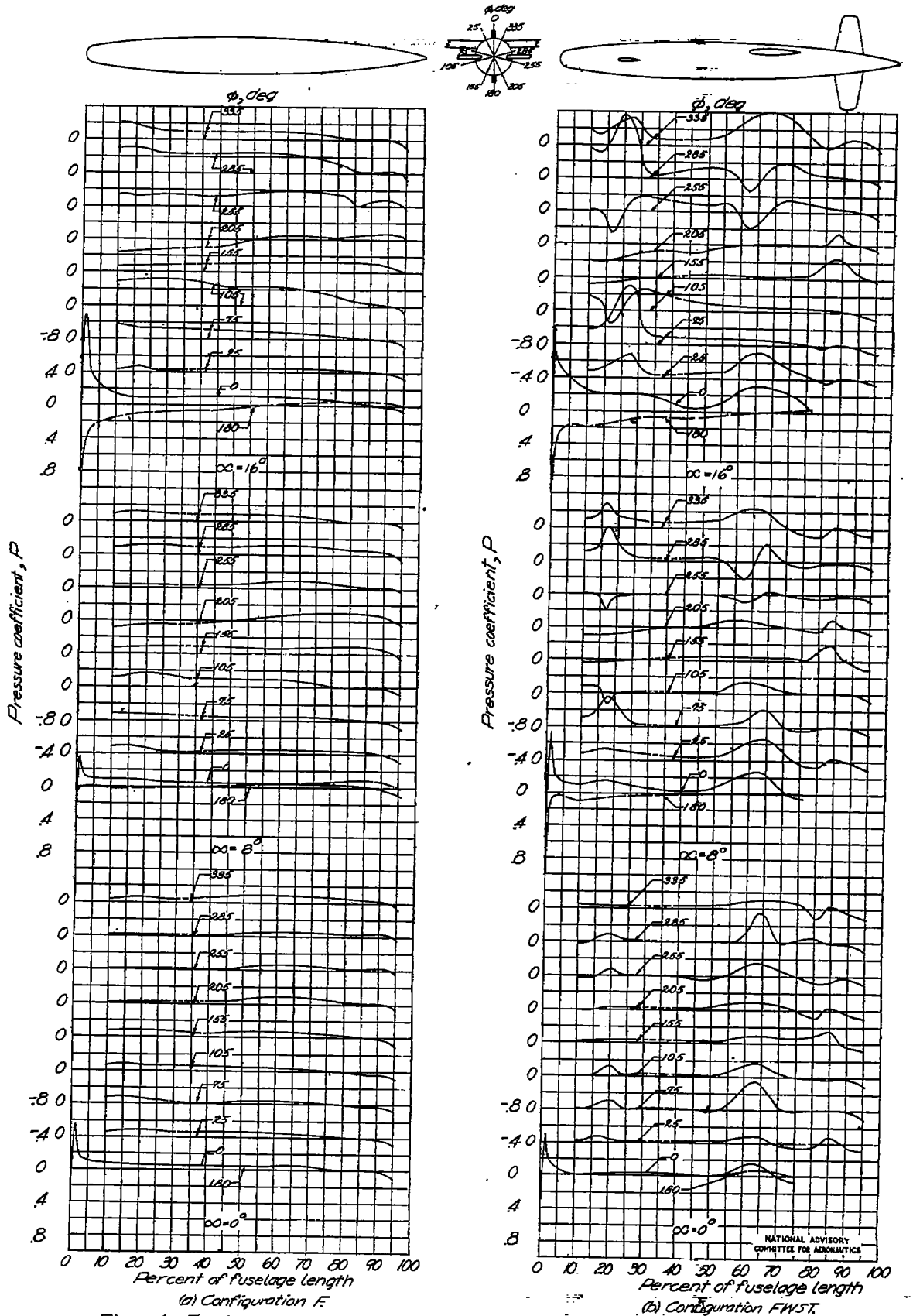

Figure 4.- Fuselage pressure distribution for several positions of the generatrix. $\Psi = 5°$.

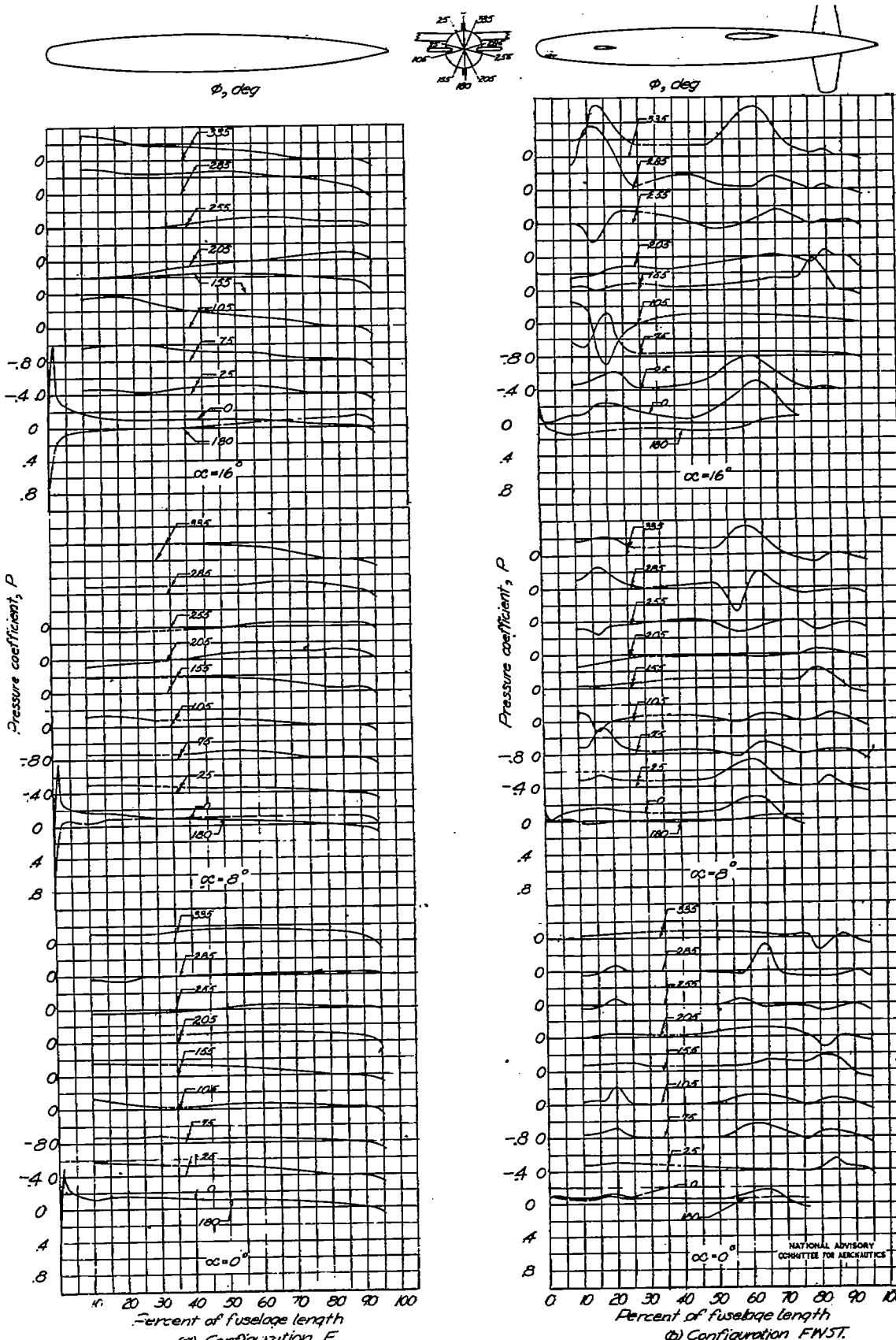

Figure 5.-Fuselage pressure distribution for several positions of the generatrix. Φ = 10°.

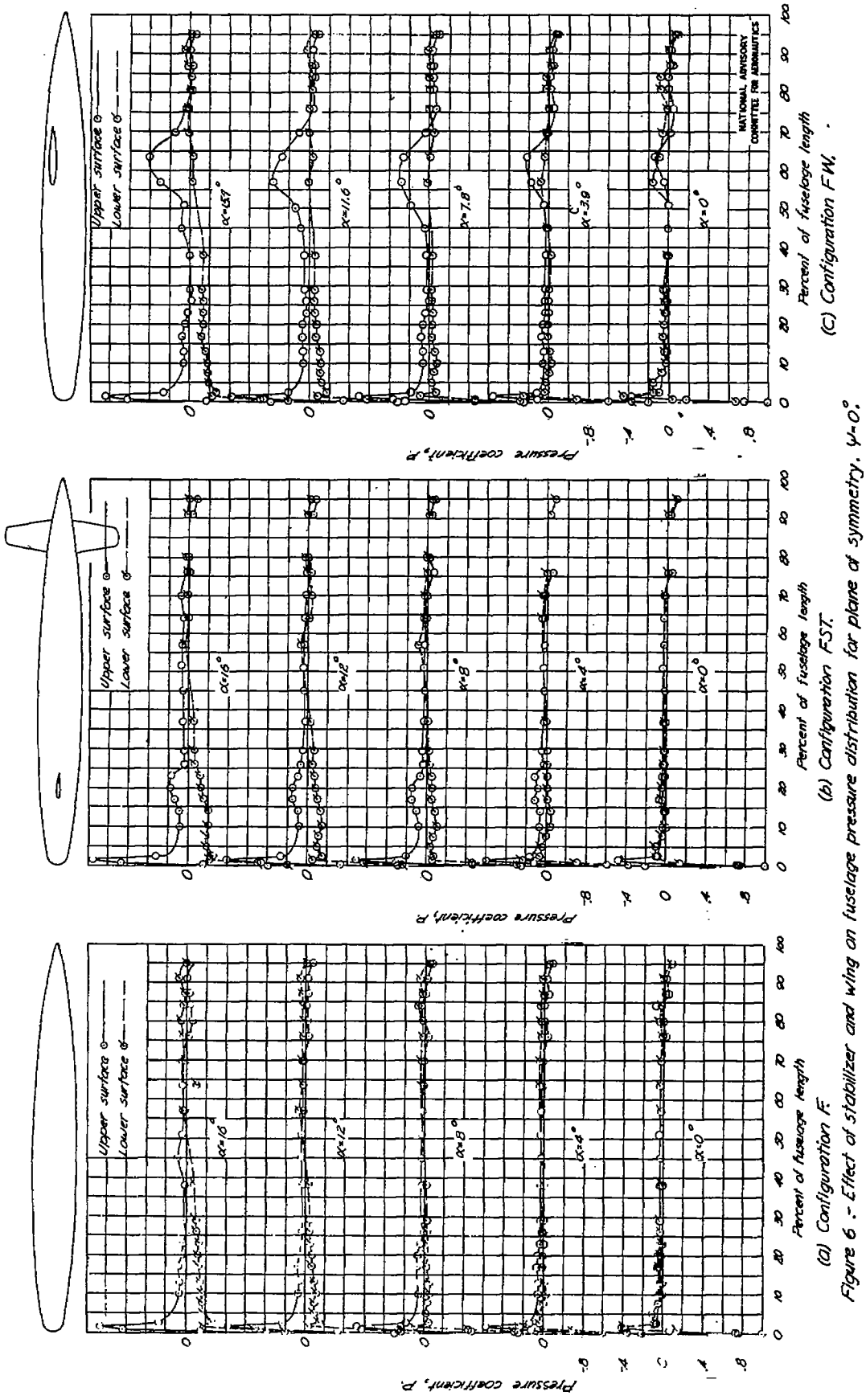

(a) Configuration F.

(b) Configuration FST.

(c) Configuration FW.

Figure 6.- Effect of stabilizer and wing on fuselage pressure distribution for plane of symmetry. $\psi=0°$.

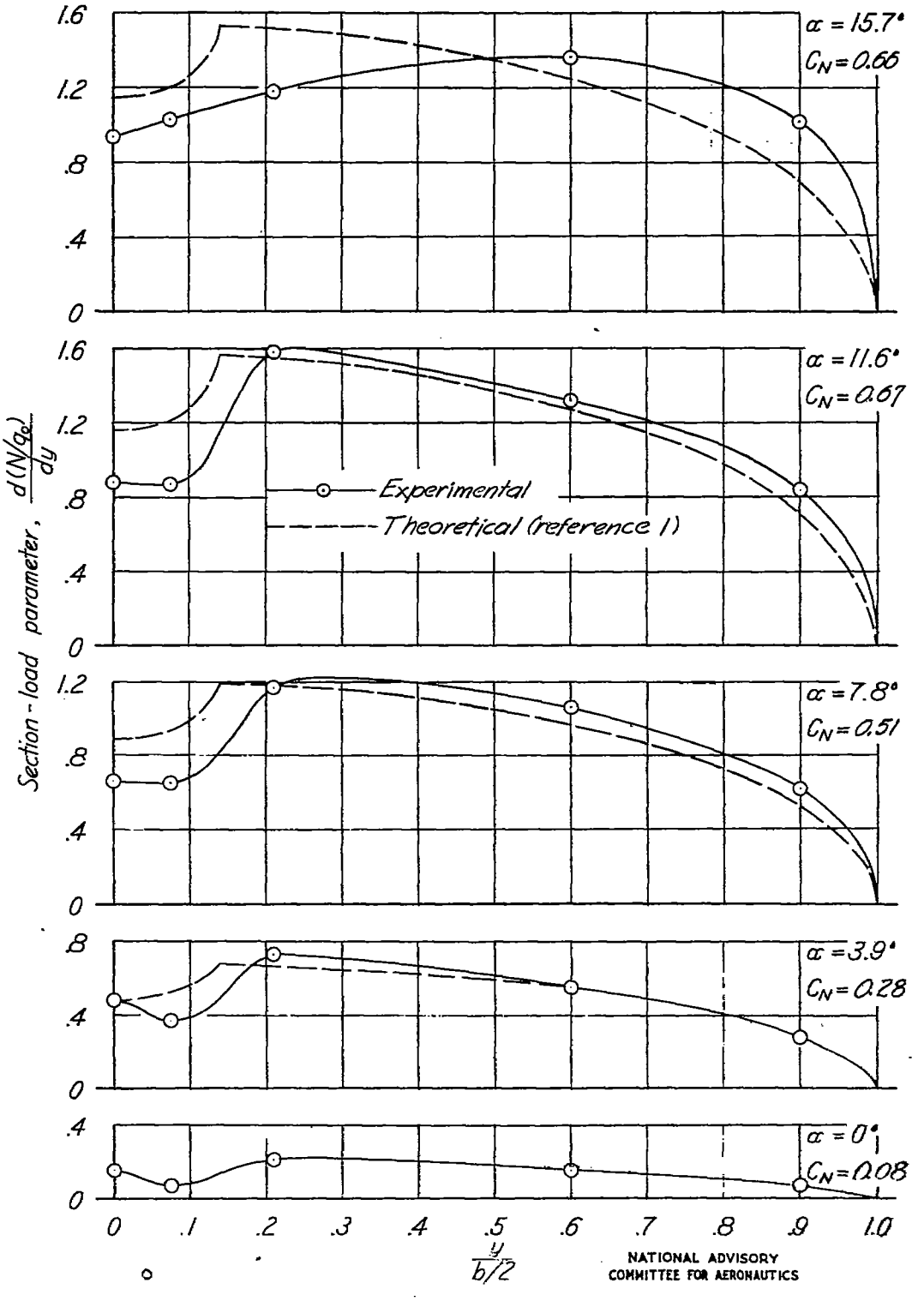

Figure 7.— Comparison of theoretical and experimental wing span loading. $\psi=0°$; configuration FWT.

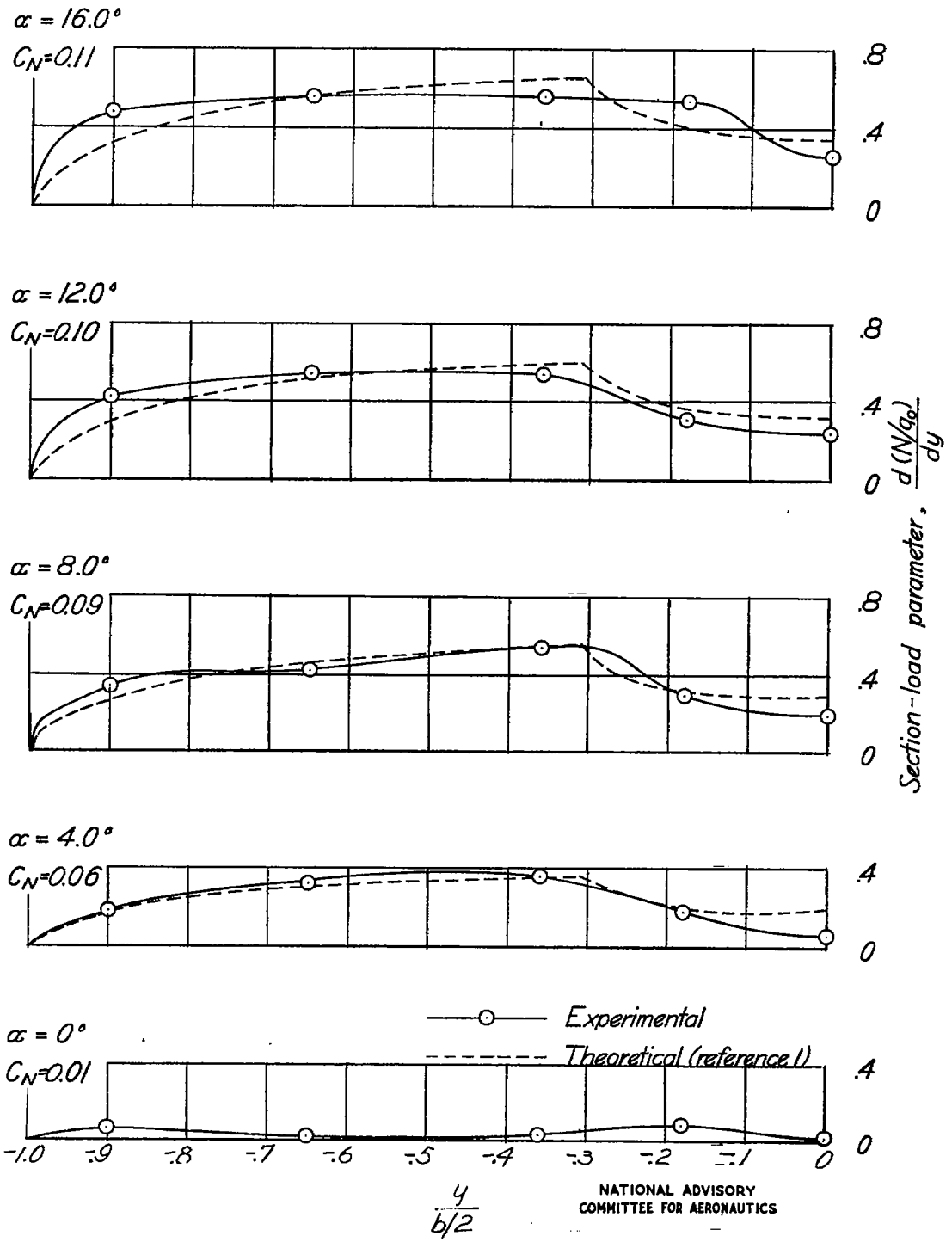

Figure 8.— Comparison of theoretical and experimental stabilizer span loading. $\psi = 0°$; configuration FST.

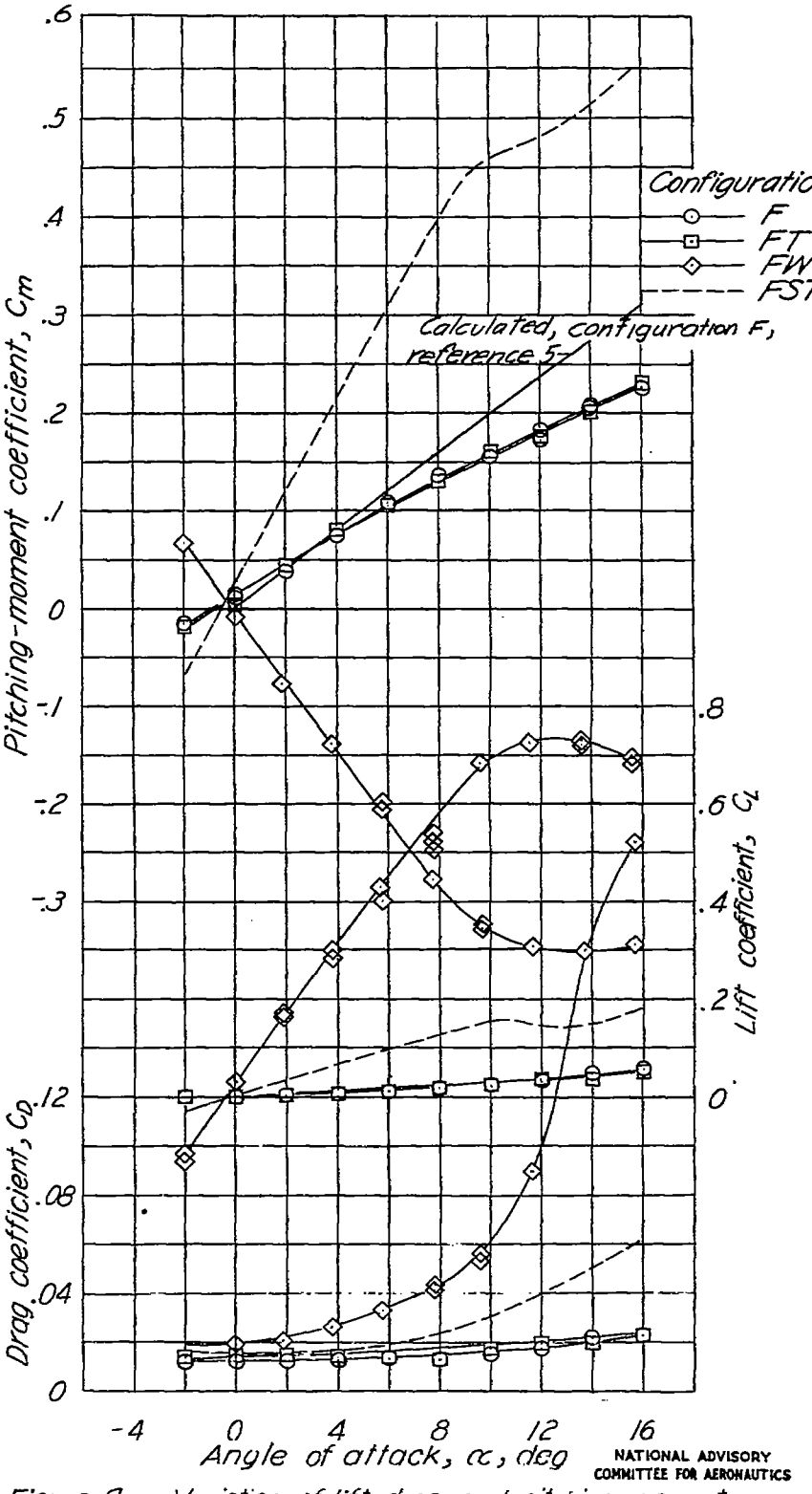

Figure 9.- Variation of lift, drag, and pitching-moment coefficients with angle of attack for several configurations. $\gamma=0°$.

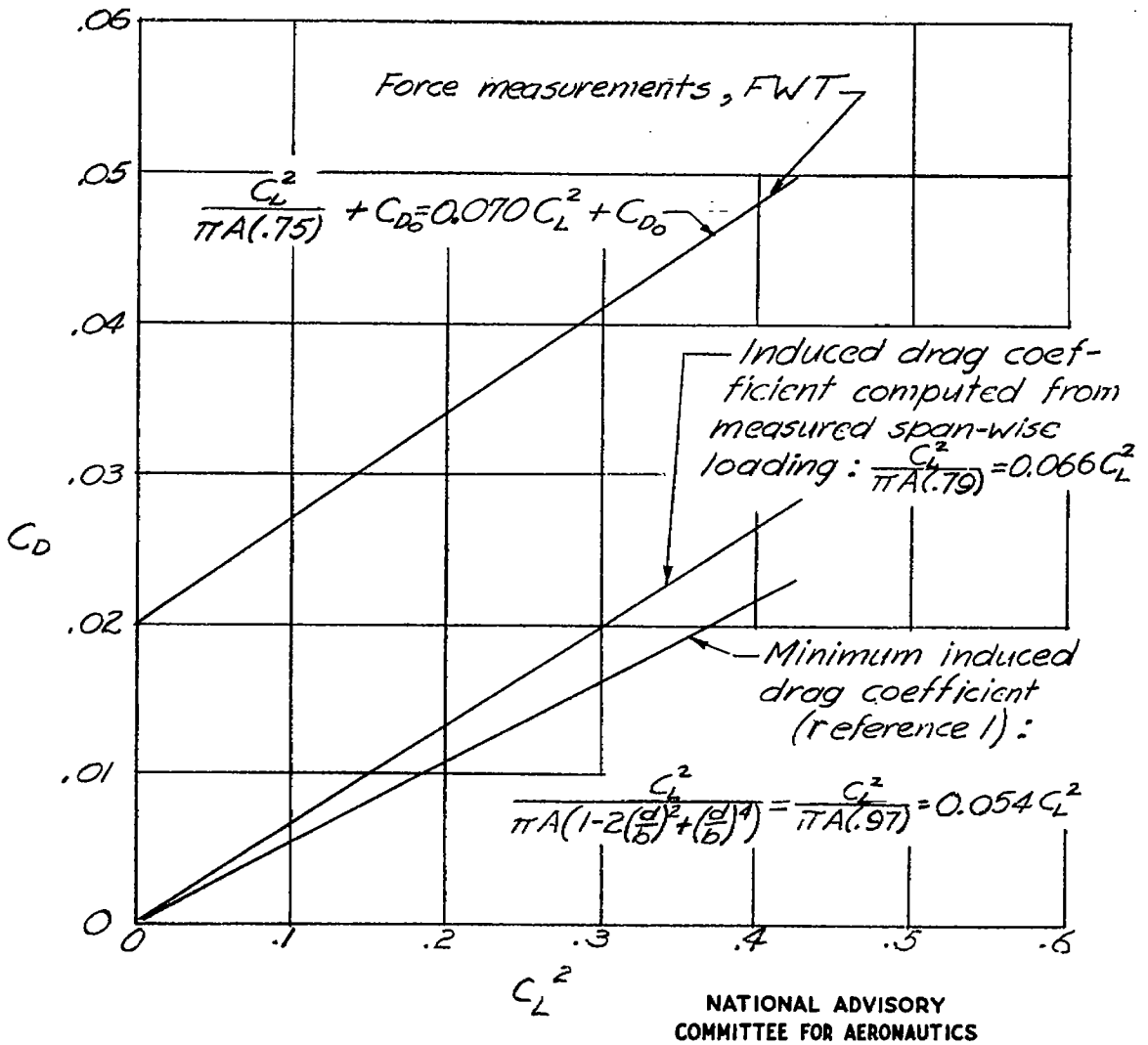

(a) Configuration FWT.

Figure 10.- Variation of drag coefficient with square of lift coefficient.

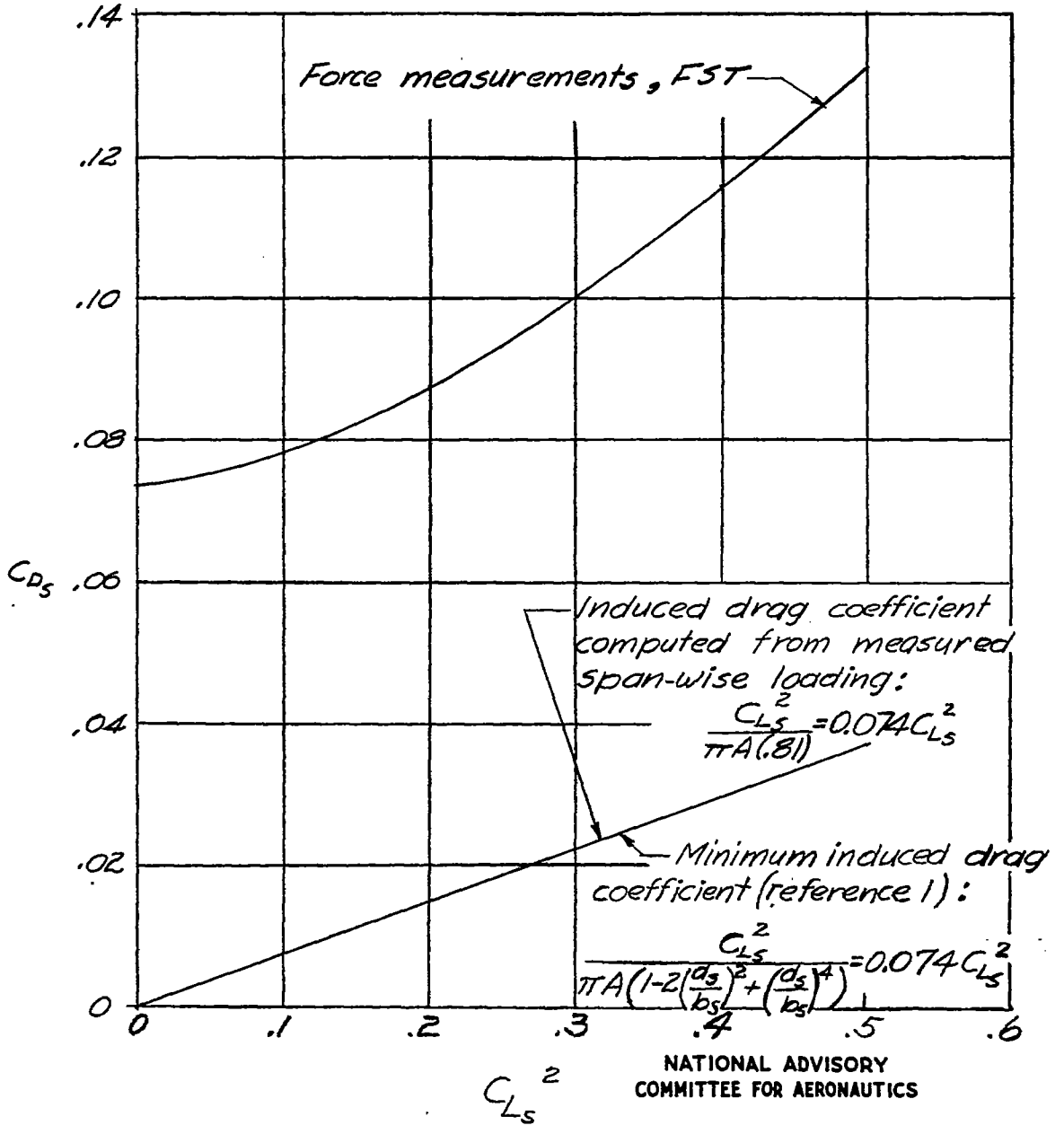

(b) Configuration FST.

Figure 10.- Concluded.